Inverse Problems and Their Regularization

Heinz W. Engl

Industrial Mathematics Institute, Johannes Kepler Universität, Altenbergerstr. 69, A-4040 Linz, Austria
engl@indmath.uni-linz.ac.at,
WWW home page: http://www.indmath.uni-linz.ac.at

1 Introduction

Inverse Problems are concerned with determining *causes* for *desired* or *observed* effects; from this formulation, it is clear that inverse problems appear frequently in all kinds of applied fields. Examples of important classes of inverse problems are

- *tomography* (cf. [57]), which is important both in medical applications and in nondestructive testing [28]
- *inverse scattering* (cf. [16], [61])
- *inverse heat conduction problems* like solving a heat equation backwards in time or "sideways" (i.e., with Cauchy data on part of the boundary) (cf. [29], [4])
- *geophysical inverse problems* like determining a spatially varying density distribution in the earth from gravity measurements (cf. [27])
- inverse problems in *imaging* like deblurring and denoising (cf. [5])
- *identification of parameters* in (partial) differential equations from interior or boundary measurements of the solution (cf. [3], [46]), the latter case appearing e.g. in *impedance tomography* ([45]).

Detailed references for these and many more classes of inverse problems can be found e.g. in [30], [21], [24],[35],[53], [49],[42],[15].

We now give one example each for inverse problems concerned with determining causes for an *observed* and a *desired* effect, respectively. Usually, in the first case, one is interested in uniqueness, since one needs a unique cause for the observation, while in the second case, where not the cause but the desired effect is important, uniqueness is not even desirable: it can be advantageous to have several possible strategies for obtaining a desired effect available. Both our examples stem from different aspects of iron and steel production:

Example 1. (cf. [59]): The blast furnace process is still the most important technology in steel production to get iron from ore. Due to the high temperatures (up to $1500°C$), measurements of any kind are impossible inside the furnace. Therefore, the development of mathematical models allowing the numerical simulation of the process is important (see [20] for a kinetic model of the blast furnace process). The problem treated in [59] has to do with operational safety: The inside lining of the furnace consists of bricks of different materials (with different thermal conductivities) and is subject to physical and chemical wear, leading to the erosion of the bricks, i.e., the thickness of the lining is decreasing. At the same time, due to variations in the working conditions of the furnace, slag may deposit; this happens mainly on the sides, but also on the bottom of the furnace, increasing the thickness of the lining.

If the lining becomes too thin, the process must be stopped to avoid a breakthrough which not only would cause tremendous damage but is also very dangerous to the staff. On the other hand, since it is problematic to reactivate a stopped furnace, to halt production entrains almost inevitably the relining of the furnace. During that time, the steel plant has to deal with an enormous loss of production of pig-iron, which may trouble even subsequent production steps, besides high expenses for the relining. Moreover, at the beginning / restart of a campaign it takes some time to get the whole process running, and the produced pig-iron is of lower quality. Altogether, long campaigns are desired, so that the process should not be stopped too early. This given, the problem is to reliably calculate the thickness of the wall in the hearth in order to stop the furnace right in time. To this purpose, temperature measurement devices are placed inside the wall when the lining is bricked. One wants to calculate the shape of the wall on the inner, inaccessible side of the furnace, based on these measurements.

Since the furnace is (essentially) rotationally symmetric, the wall of the furnace in the region considered can be modelled in cylindrical coordinates. The (reasonable) assumption of stationarity and rotational symmetry lead to the following nonlinear elliptic equation in the radial and height variables (since the temperature u does not depend on the angular variable):

$$\frac{\partial}{\partial r}(\lambda\frac{\partial u}{\partial r}) + \frac{\lambda}{r}\cdot\frac{\partial u}{\partial r} + \frac{\partial}{\partial z}(\lambda\frac{\partial u}{\partial z}) = 0 \quad \text{in } \Omega, \tag{1}$$

where Ω denotes a radial cross-section of the wall (see Figure 1) with the boundary $\Gamma = \Gamma_1 \cup \Gamma_2 \cup \Gamma_3 \cup \Gamma_4$.

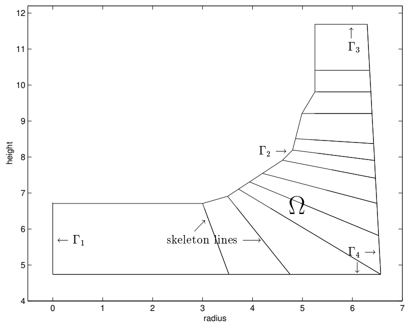

Fig. 1. Sketch of the furnace: two-dimensional, rotationally symmetric

The heat conductivity depends on the material, which changes over Ω (since Ω is covered by different types of brick and possibly slag), and hence on position, and also on the temperature:

$$\lambda = \lambda(r, z, u). \tag{2}$$

Due to rotational symmetry and the fact that the lining continues past Γ_3, we have the boundary conditions

$$\frac{\partial u}{\partial n} = 0 \quad \text{on} \quad \Gamma_1 \quad \text{and on} \quad \Gamma_3. \tag{3}$$

The outer surface is cooled by water with temperature T_w, which leads to the boundary condition

$$-\lambda \frac{\partial u}{\partial n} = \alpha_0 \cdot (u - T_w) \quad on \quad \Gamma_4 \tag{4}$$

with a (measurable) heat transfer coefficient α_0. At the inner surface of the wall, an analogous condition

$$-\lambda \frac{\partial u}{\partial n} = \alpha \cdot (u - T_i) \quad \text{on} \quad \Gamma_2 \tag{5}$$

holds, where the heat transfer coefficient α depends on the actual material present at Γ_2 and T_i is the interior temperature of the furnace (i.e., of molten iron).

If Ω, i.e., the shape of the inside lining, were known, we could solve (1)-(5), which is called the *direct problem*, and compute the temperature field u in Ω. Especially, we could predict the temperatures

$$\tilde{u}_j := u(x_j), j \in \{1, \cdots, m\} \tag{6}$$

measured by thermocouples located at finitely many points $x_j \in \Omega$. Our *inverse problem* now is to determine the inner contour Γ_2 and hence Ω from measurements of $\tilde{u}_j$. Note that this problem could also be viewed as a shape optimization or as a free boundary problem.

Of course, one cannot expect uniqueness in this setup, since one has only finitely many data $\tilde{u}_1, \cdots, \tilde{u}_m$ to determine the curve Γ_2. One could consider the corresponding infinite-dimensional problem of determining Γ_2 from temperature values at a whole curve inside Ω or, which is more practical, describe Γ_2 by finitely many parameters. In [59], Γ_2 has been described by the distances p_i from the outer contour Γ_4 along the skeleton lines (see Figure 1). If we denote, for $p = (p_1, \cdots, p_n)$, by u_p the temperature field determined by (1)-(5)with Γ_2 (and hence Ω) determined by p, then our inverse problem can be reformulated as the least squares problem

$$\Phi(p) := \sum_{j=1}^{m} (u_p(x_j) - \tilde{u}_j)^2 \to \min., \quad p \in C, \tag{7}$$

where C symbolizes constraints on p (see [59]). It turns out, however, that this least squares problem is quite unstable: Figure 2 shows two domains Ω, which are markedly different, but lead to about the same value for Φ. This can be remedied by *regularization*, which will be explained below.

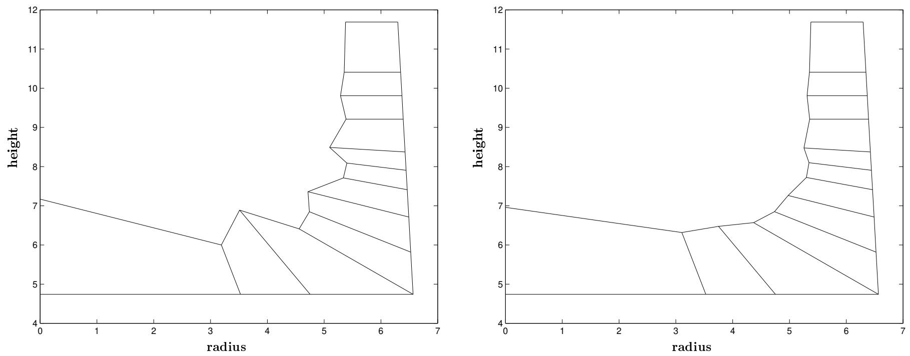

Fig. 2. Two possible solutions, the first one being not very realistic, while the second one is physically reasonable

Note that uniqueness is of importance here, since one wants to find a unique inner lining which gives information about the current status of the furnace, and not several (or even infinitely many) possible inner contours. Of course, with finitely many data, one can at best obtain uniqueness for finitely many parameters describing Γ_2, i.e., one needs some a-priori assumptions about Γ_2.

Example 2. (cf. [33]): At the beginning of the continuous casting process the liquid steel is cooled in a water–cooled mould to form a solidified shell which can support the liquid pool at the mould exit. Typical temperatures at the end of the mould are 1100 °C at the strand surface and 1550 °C in the center of the strand. Since steel does not solidify at a fixed temperature, but over a temperature interval, there is a mushy region where the steel is neither completely solid nor completely liquid. Steel grades used in continuous casting are completely solid below a temperature T_{SOLID} of 1350 to 1500 °C, and the solidification starts at a temperature T_{LIQUID} between 1450 and 1525 °C (strongly depending on the content of alloying elements). Liquid steel is provided with a temperature which is typically 30 °C higher than the liquidus temperature. In the mushy region segregation occurs, depending on parameters like content of alloying elements, solidification rate and superheat temperature.

After the mould, the cooling process is continued in secondary cooling zones by spraying water onto the strand. Near the point of final solidification (*crater end*) the segregation effects are pronounced. In this region the temperature gradient in the center of the strand is much larger than the temperature gradient at the strand surface. The increased shrinkage of the strand center causes rest melt enriched with impurifications to flow towards the crater end which decreases the product quality. One possibility to reduce center segregation is to compensate shrinkage of the strand center by slightly reducing the strand thickness at the crater end. This process is called *soft–reduction*.

In order to make soft–reduction work efficiently, one has to be able to find a cooling strategy which, for a known but variable casting speed, makes sure that the crater end always remains in the soft–reduction zone.

For a constant casting speed, the more general inverse problem of controlling the whole solidification front by secondary cooling was considered e.g. in [26]. The problem for a variable casting speed, even if one only needs to control the location of the crater end, is much more complicated and complex since no cross–section of the steel strand can now be considered independently from the others. In practice, a change of the casting speed is e.g. necessary if there are problems in the steel making or in the hot rolling process. It also could be that the casting process has to stop for a short time and then start again to make it possible to change the setup of the casting machine, e.g., the width.

The control parameter for this problem is the amount of water sprayed onto the strand in the secondary cooling zones. For technical reasons the amount of water sprayed onto the strand has to be constant in each cooling zone (there are typically six cooling zones), but can vary in time; thus one has to admit piecewise constant, i.e., non–smooth heat transfer functions in the mathematical model. Furthermore, there are upper and lower bounds for the amount of water.

In [33], the problem is described in Lagrangian coordinates. The strand moves in the casting direction z with the casting speed $v(t)$, y is the direction of width and x the direction of thickness of the strand in which the spray cooling takes place. It is justified to neglect the heat conduction in the casting direction since it is much smaller than the heat conduction in the directions perpendicular to it. If the strand width is much larger than the strand thickness, which is fulfilled for slabs whose cross–section is around 120×25 cm, it is also justified to assume that for a fixed cross–section the temperature in the area near the center of the strand width–direction only depends on the x–coordinate and time. If d is the strand thickness and if the cooling is done in a symmetric way, the temperature is symmetric with respect to the plane $x = d/2$, provided the initial temperature $f(x,t)$ fulfills this condition. Therefore, the partial derivative u_x of the temperature u vanishes for $x = d/2$.

The amount of cooling water with temperature U_w sprayed onto the strand in the secondary cooling region enters into the boundary conditions via a heat transfer function $g(z,t)$. The model also includes cooling due to radiation (U_a being the temperature of the surrounding air).

The material parameters of steel primarily relevant for the problem are the thermal conductivity $k(u)$, the density $\rho(u)$ and the specific heat $c(u)$, which all depend on the temperature $u = u(x,z,t)$. σ is the Stefan–Boltzmann constant and ϵ a further material parameter that depends on the steel grade.

With these notations, the temperature field is described by the following mathematical model:

$$[k(u)u_x]_x = \rho(u)c(u)u_t \tag{8}$$
$$u(x, z = -\textstyle\int_0^t v(\tau)\, d\tau, t) = f(x,t) \tag{9}$$
$$u_x(d/2, z, t) = 0 \tag{10}$$
$$\begin{aligned} k(u(0,z,t))u_x(0,z,t) = g(z + \textstyle\int_0^t v(\tau)\, d\tau, t)(u(0,z,t) - U_w) \\ + \sigma\epsilon(u^4(0,z,t) - U_a^4). \end{aligned} \tag{11}$$

The Eulerial coordinate 0 describes the lower end of the mould. At time t the cross–section with Lagrangian coordinate $z = -\int_0^t v(\tau)\, d\tau$ passes this end of the mould. The temperature $f(x,t)$ at the end of the mould in (9) for this cross–section can be computed by calculating the temperature in the mould. It is assumed that at the beginning of the mould there is a constant initial temperature. The function f depends on time since the casting speed is not constant, so that different cross–sections remain in the mould for different amounts of time and thus cool down in a different way. $z + \int_0^t v(\tau)\, d\tau$ is the Eulerian coordinate of the cross–section with Lagrangian coordinate z at time t. This is used to compute the cooling for the cross–section z in (11).

If the material parameters k, ρ and c, the casting speed v as a function of time, the initial temperature f and the heat transfer function g are known, we call the problem of solving (8)–(11) for the temperature u the *direct problem*. The neglection of the heat conduction in the casting direction implies that one can look at each cross–section of the strand separately for solving the direct problem: The temperatures of different cross–sections evolve independently from each other. From the solution of the direct problem, the point of complete solidification of each cross–section can be obtained. Note that mathematical questions like existence and uniqueness of a solution of (8)–(11) are non–trivial due to the fact that g is piecewise constant (see [34]).

The problem to find a cooling strategy that makes sure that the crater end always remains within the soft–reduction zone amounts to solving the following *inverse problem*: If the material parameters, the casting speed, the initial temperature are known and the position of the soft–reduction zone is prescribed, a heat transfer function g has to be computed in such a way that with this cooling, the resulting solution of the direct problem is such that the crater end of each cross–section of the strand is in the given region defined by the soft–reduction zone.

In the direct problem one can look at each cross–section separately to compute the temperature if one neglects the heat conduction in the casting direction. This decoupling could also be done for the inverse problem if the casting speed would be constant: In this case, one could compute a time–independent heat transfer function g for one cross–section and use it also for the other cross–sections. In the present case, however, one cannot use a time–independent heat transfer function since the casting speed varies. But then, since the heat transfer function has to be piecewise constant in space and time, one has to look at all cross–sections simultaneously. This increases the complexity of the problem considerably and requires to look for an efficient algorithm to solve the inverse problem and hence also the direct problem.

Note that for this inverse problem, uniqueness is not important: it is fine, maybe even advantageous, if these are several cooling strategies leading to the *desired effect* to keep the crater and within the soft reduction zone.

The mathematical models for inverse problems usually are not *well-posed* in the sense of Hadamard, i.e., they do not fulfill the postulates that for all admissible data,

– a solution *exists*,
– the solution is *unique*,
– the solution *depends continuously* on the data.

Thus, inverse problems are the source for *ill-posed* problems, which is the reason that the analysis and numerics of such problems has been extensively studied in recent years. Of special importance is the instability (discontinuous dependence on the data) usually connected with ill–posedness, since it obviously creates severe numerical problems: algorithms one uses for well–posed problems usually do not work for ill–posed problems unless special features are added which remedy the instability; these lead to *regularization methods* which we will discuss in this paper. Numerical examples which clearly show the instability of traditional methods (using no regularization) applied to inverse problems can be found for a deconvolution problem arising in physical chemistry in [51], for inverse scattering in [18] (see also [17]).

This instability in the inverse problem is usually connected with a smoothing effect in the *direct* (*forward*) *problem*: Convolution smoothes, so does heat conduction forward in time, which means that rough details are smoothed out in the forward problem; this in turn has the effect that in the inverse problem, small errors may be amplified into large artefacts.

Both examples treated above were *nonlinear* inverse problems, as are many inverse problems arising in practice. Also, note that even if the corresponding direct problem is linear, an inverse problem connected with it may be nonlinear, as is the case e.g. in the problem of identifying a parameter $a = a(x)$ from the values of the solution of the problem

$$\begin{aligned} (au_x)_x &= f \quad \text{in} \quad [0,1] \\ u_x(0) &= u(1) = 0 : \end{aligned} \tag{12}$$

Its solution is

$$a(x) = \frac{1}{u_x(x)} \int_0^x f(s)ds$$

and hence depends in a nonlinear way on u. Note also that it involves differentiating the data u, which is unstable.

Nevertheless, we first present aspects of the theory of *linear* inverse problems, since it is more complete and, of course, easier. A prototype of linear inverse problems are *integral equations of the first kind*

$$\int_G k(s,t)x(t)dt = f(s) \tag{13}$$

for an unknown function x (cf. [30]).

2 Regularization of Linear Ill–Posed Problems

We phrase linear ill-posed problems in the abstract setting of linear operator equations

$$Tx = y \tag{14}$$

with a bounded linear operator T between Hilbert spaces X and Y, which especially includes first-kind integral equations like (13). As concept of solution we use that of a *best–approximate solution*, which is a minimizer of the residual $\|Tx - y\|$ and minimizes $\|x\|$ among all minimizers of the residual. We thus concentrate on the stability issue, doing away with non–uniqueness. The operator $T^\dagger$ which maps $y \in D(T^\dagger)$ to the best–approximate solution of (14) is known as the *Moore-Penrose (generalized) inverse* of T (see e.g. [56], [36]). Its domain is

$$D(T^\dagger) = R(T) \dot{+} R(T)^\perp, \tag{15}$$

and $T^\dagger$ is bounded if and only if $R(T)$ is closed. Hence, the problem of determining the best–approximate solution of (14) is well–posed if and only if $R(T)$ is closed, which is not the case if T is compact and $\dim R(T) = \infty$. Hence, *integral equations of the first kind* with a non–degenerate kernel such that the integral operator is compact are *always ill–posed.*

If T is compact with singular system $\{\sigma_n; u_n, v_n\}$, then $y \in D(T^\dagger)$ if and only if

$$\sum_{n=1}^{\infty} \frac{|\langle y, v_n \rangle|^2}{\sigma_n^2} < \infty, \tag{16}$$

which is called the *Picard criterion*; then, the best–approximate solution of (14) has the series representation

$$T^\dagger y = \sum_{n=1}^{\infty} \frac{\langle y, v_n \rangle}{\sigma_n} u_n. \tag{17}$$

This formula clearly shows the instability: errors in Fourier components of y with respect to v_n, i.e., in $\langle y, v_n \rangle$, are amplified by $\frac{1}{\sigma_n}$, which grows without bound since $\lim_{n\to\infty} \sigma_n = 0$ (if $\dim R(T) = \infty$). This error amplification is the worse the faster the σ_n decay to 0, i.e., for the case of integral operators, the smoother the kernel is! Thus, integral equations of the first kind with a smooth kernel are *severely ill–posed*, the decay rate of the singular values can be used to quantify ill-posedness.

The formula (17) also indicates how one can stabilize (*regularize*) the problem: using that $Tu_n = \sigma_n v_n$, (17) can also be written in symmetric form as

$$T^\dagger y = (T^*T)^\dagger T^* y = \sum_{n=1}^{\infty} \frac{\langle T^* y, u_n \rangle}{\sigma_n^2} u_n. \tag{18}$$

We now replace the amplification factors $\frac{1}{\sigma_n^2}$ by a *filtered* version $U_\alpha(\sigma_n^2)$, where the filter function U_α is such that for $\alpha > 0, U_\alpha$ is piecewise continuous on $[0, +\infty[$ (especially, does not have a pole at 0) and that

$$\lim_{\alpha \to 0} U_\alpha(\lambda) = \frac{1}{\lambda} \quad \text{for} \quad \lambda > 0; \tag{19}$$

this convergence is pointwise only, and $|\lambda \cdot U_\alpha(\lambda)|$ is required to stay bounded.

As *regularized solution* (with noisy data y^δ fulfilling $\|y - y^\delta\| \le \delta$) we take:

$$x_\alpha^\delta := \sum_{n=1}^{\infty} U_\alpha(\sigma_n^2) \cdot \langle T^* y, u_n \rangle u_n = \sum_{n=1}^{\infty} \sigma_n \cdot U_\alpha(\sigma_n^2) \cdot \langle y, v_n \rangle u_n. \tag{20}$$

The constant α is called the *regularization parameter.*

Different choices of the filter function U_α now lead to different regularization methods: E.g., for

$$U_\alpha(\lambda) := \frac{1}{\alpha + \lambda} \tag{21}$$

we obtain *Tikhonov regularization*

$$x_\alpha^\delta = \sum_{n=1}^{\infty} \frac{\sigma_n}{\alpha + \sigma_n^2} \langle y^\delta, v_n \rangle u_n = (\alpha I + T^*T)^{-1} T^* y^\delta, \tag{22}$$

which can also be characterized in variational form as minimizer of the functional

$$x \to \|Tx - y^\delta\|^2 + \alpha \|x\|^2. \tag{23}$$

See [30] for other choices of filter functions U_α leading to different regularization methods.

In any regularization method, the choice of the *regularization parameter* α is crucial. As can be seen from (23), it represents a compromise between accuracy and stability: if α is small, the residual term $\|Tx - y^\delta\|^2$ dominates, so that minimizers tend to lead to a small residual, but may have a large norm; if the norm contains derivatives, e.g., is the H^2-norm, this means that solutions tend to be heavily oscillating. Such oscillations can be seen (in a nonlinear inverse problem) the left picture in Figure 2 above; note that this picture comes from minimizing the least-squares functional (7) without a regularization term.

One distinguishes between two classes of parameter choice rules: In *a-priori rules*, one chooses the regularization parameter as a function of the noise level only, i.e., $\alpha = \alpha(\delta)$, while in *a-posteriori rules*, one uses the noise level and the actual data, i.e., $\alpha = \alpha(\delta, y^\delta)$. A classical a-posteriori rule is the so-called *discrepancy principle*, where α is chosen such that

$$\|Tx_\alpha^\delta - y^\delta\| = C\delta \tag{24}$$

holds (with some $C > 1$), which is a nonlinear equation in α.

One can show (see [30]) that *error-free* strategies, where $\alpha = \alpha(y^\delta)$ does not depend on δ, cannot lead to convergence as $\delta \to 0$ in the sense that $\lim\limits_{\delta\to 0} x_\alpha^\delta = T^\dagger y$ for all y^δ with $\|y - y^\delta\| \leq \delta$. These error-free strategies include the popular methods of generalized cross-validation ([71]) and the *L-curve method* ([40]); for its non–convergence, see [23] and [70].

Crucial questions in applying regularization methods are convergence *rates* and how to choose regularization parameters to obtain optimal convergence rates. By convergence rates we mean rates for the worst-case error

$$\sup\{\,\|x_\alpha^\delta - T^\dagger y\| \,/\, \|y - y^\delta\| \leq \delta\} \tag{25}$$

for $\delta \to 0$ and $\alpha = \alpha(\delta)$ or $\alpha = \alpha(\delta, y^\delta)$ chosen appropriately. For an ill–posed problem, no uniform rate valid for all $y \in Y$ can be given ([67]), such rates can only be given on compact subsets of X (cf. [52]). An example of this are convergence rates valid under *source conditions* (with a $\nu > 0$)

$$T^\dagger y \in R((T^*T)^\nu), \tag{26}$$

which can, using a singular system, also be written as

$$\sum_{n=1}^{\infty} \frac{|\langle\, y, v_n \,\rangle|^2}{\sigma_n^{2+4\nu}} < \infty, \tag{27}$$

which puts the Picard criterion into a scale of such conditions (for $\nu = 0$): under the condition (26), which can be (due to the fact that usually T is smoothing) thought of as (abstract) a–priori smoothness condition, Tikhonov regularization converges with the rate

$$\|x_\alpha^\delta - T^\dagger y\| = O(\delta^{\frac{2\nu}{1+2\nu}}) \tag{28}$$

for the a–priori choice

$$\alpha \sim \delta^{\frac{2}{1+2\nu}} \tag{29}$$

and $\nu \leq 1$.

This (as it turns out, optimal under (26)) rate is also achieved with the a–posteriori parameter choice (24), but only for $\nu \leq \frac{1}{2}$. For a–posteriori parameter choice rules that always lead to optimal convergence rates see [22] and [63].

The total error of a regularization method has the form outlined in Fig. 3: the regularization error $\|x_\alpha^0 - T^\dagger y\|$ goes to 0 as $\alpha \to 0$, while the propagated data error $\|x_\alpha^0 - x_\alpha^\delta\|$ grows without bound as $\alpha \to 0$; the method of [22] for optimally choosing the regularization parameter is based on minimizing the total error, which is not as easy as it sounds since the curves in Figure 3 are not computable unless one knows the exact solution of the problem.

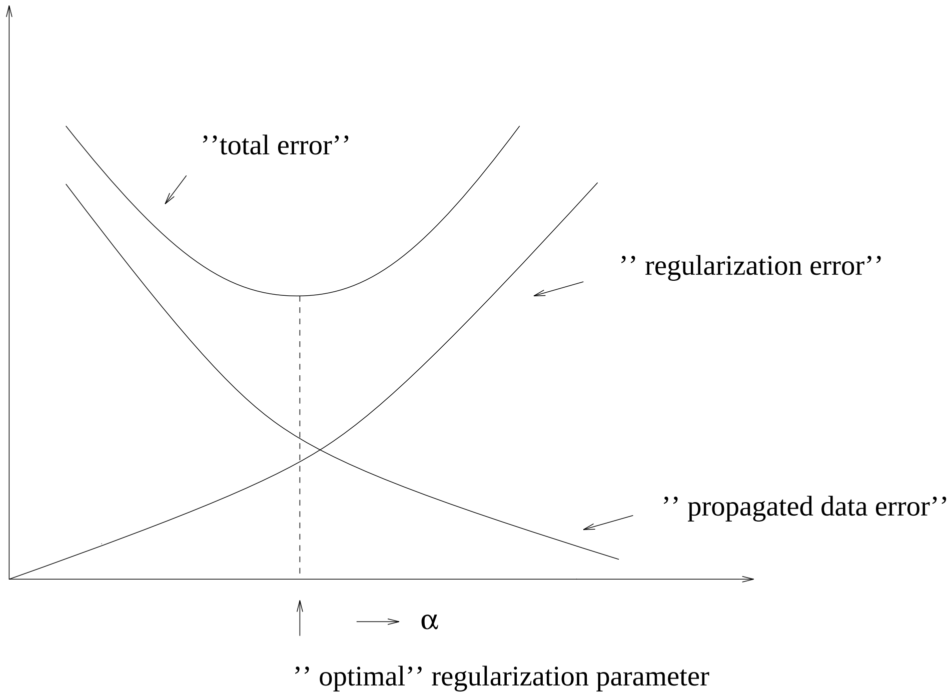

Fig. 3. Typical error behaviour

Methods which are closely related to regularization methods are *mollifier methods*, where one looks for a smoothed version of the solution, cf. [55]. While these are still linear methods, there are also *nonlinear methods* for solving linear ill–posed problems, e.g., the *Backus–Gilbert method* ([1], [50]) and the *conjugate gradient method* ([9], [54], [37]). For details about these methods and other aspects we do not touch here (like the non–compact case and numerical aspects in the framework of combining regularization in Hilbert space with projection into finite-dimensional spaces) see [30]. We mention in closing that there is a close connection between regularization and approximation by neural networks (cf. [12] and the references quoted there).

3 Nonlinear Ill–Posed Problems

We describe nonlinear ill–posed problems as nonlinear operator equations

$$F(x) = y, \tag{30}$$

where F maps a domain $D(F)$ in a Hilbert space X into a Hilbert space Y. The basic assumptions for a reasonable theory are that F is continuous and weakly sequentially closed (cf. [25]). In contrast to linear problems, F is usually not explicitely given in models on nonlinear inverse problems; it symbolizes the operator describing the direct problem, the *forward map*. E.g., in the situation of Example 1, F is the operator mapping the inner contour Γ_2 to the observed temperatures u on a curve in Ω (if we consider the infinite-dimensional problem) or the operator mapping the parameter vector p (which in turn determines Γ_2) to the observation vector $(\tilde{u}_1, \cdots, \tilde{u}_m)$. Although, in the latter situation, F maps a finite-dimensional vector to another finite-dimensional vector, it involves solving the infinite-dimensional problem (1)-(5).

In the situation of Example 2, F could be the operator mapping a given cooling strategy to the distance (as a function of time) from the crater end to the soft-reduction zone, $y \equiv 0$.

In the simple parameter identification (12), F is the *parameter-to-solution-map* mapping a to the solution u of the boundary value problem (12).

Like in the linear case, we introduce a generalized solution concept (for simplicity, for the case that y is *attainable*, i.e., (30) has a solution; see [8] for the non-attainable case): For $x^* \in X$, we call a solution of (30) which minimizes $\|x - x^*\|$ among all solutions an x^**-minimum–norm solution* ($x^* - MNS$) of (30); neither existence nor uniqueness are guaranteed in the nonlinear case. The choice of x^*, which will also appear in algorithms, is crucial; it should include available a–priori information like positions of singularities in x if they happen to be available.

For the question when a nonlinear equation (30) is ill–posed, we refer to [25]; like in the linear case, compactness (and some kind of non–degeneracy) of F implies ill–posedness.

The regularization methods for linear problems based on spectral theory described in Section 2 cannot be directly carried over to the nonlinear setting; however, Tikhonov regularization in its variational form of minimizing the functional (23) makes also sense for a nonlinear problem: For noisy data y^δ with $\|y - y^\delta\| \leq \delta$, we denote by x_α^δ *any* global solution of the minimization problem

$$\|F(x) - y^\delta\|^2 + \alpha\|x - x^*\|^2 \to \min . \text{ over } D(F). \tag{31}$$

Minimizers always exist for $\alpha > 0$, but need not be unique. Hence, convergence has to be understood in an appropriate set–valued sense (cf.[68]).

The basic result about convergence rates for solutions of (31) says that, under a Lipschitz condition on F' (assumed to exists as Fréchet derivative), x_α^δ converges to an x^*-MNS $x^\dagger$ of (30) with rate $O(\sqrt{\delta})$ if $\alpha \sim \delta$ and a source condition

$$x^\dagger - x^* = F'(x^\dagger)^* w \tag{32}$$

holds with a sufficiently small w (see [25]). Formally, this condition and the obtained convergence rate correspond to (26) and (28) for $\nu = \frac{1}{2}$, respectively. Again, (32) is an abstract smoothness condition for the *difference* between the true solution $x^\dagger$ and the a–priori guess x^* used in the algorithm; this underpins the remark made above that all known rough details of $x^\dagger$ should be put into the a–priori guess x^*.

Example 1, continued: In [59], Tikhonov regularization has been applied to stably solving the inverse problem. The least squares minimization problem (7) is replaced by

$$\sum_{j=1}^{m} (u_p(x_j) - \tilde{u}_j)^2 + \alpha \sum_{j\equiv 1}^{n+1} (\psi_j(p) - \psi_{j-1}(p))^2 \to \min ., p \in C, \tag{33}$$

with $\psi_0(p) = \psi_{n+1}(p) = \frac{\pi}{2}$ and $\psi_j(p)(j = 1, \cdots, n)$ being the angle between the j-tn skeleton line and Γ_2 (see Figure 1). This regularization term penalizes oscillations in Γ_2 as those in the left picture of Figure 2. We quote a result obtained in [59] with this regularization method:

In each picture in Figure 4, the dashed line is the starting contour, the continuous line is the solution calculated by the regularization algorithm, and the third line (-·-)is the "true solution" which was used to generate the data, which were then corrupted by 10 % noise. The boxes show the measurement points. The pictures show that without regularization, no useful solution can be obtained, while regularization yields quite good results (considering the high noise level). The unusual values for α result from the scaling of the problem.

We finally remark that the same practical problem was also treated in [69] for the simple case of a constant heat conductivity; instead of Tikhonov regularization, Kalman filtering was used there.

A basic disadvantage of Tikhonov regularization for nonlinear problems is that as opposed to the linear case, the functional in (31) need no longer be convex, so that it is difficult to minimize it (see [14] for a case where this is still possible).This fact makes iterative methods an attractive alternative:

A natural candidate for an iterative method for solving (30) would be Newton's method, where the $(n+1)$-st iterate x_{n+1} is determined by the linear equation

$$F'(x_n)(x_{n+1} - x_n) = -(F(x_n) - y) \tag{34}$$

or (to avoid existence problems as far as possible) by the corresponding normal equation

$$F'(x_n)^* F'(x_n)(x_{n+1} - x_n) = -F'(x_n)^*(F(x_n) - y). \tag{35}$$

However, if F is compact, so is $F'(x_n)$, so that the linear problems (34) and (35) are ill–posed. In order to make these linear problems well–posed, the operator $F'(x_n)^* F'(x_n)$ has to be replaced by an operator which has a bounded inverse.

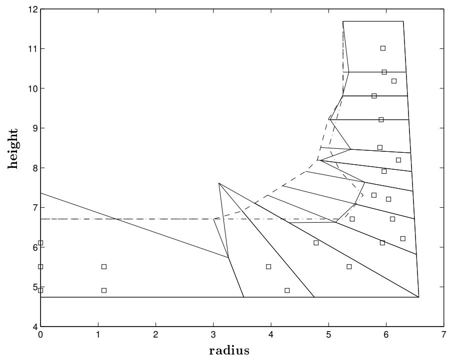

$\alpha = 0$

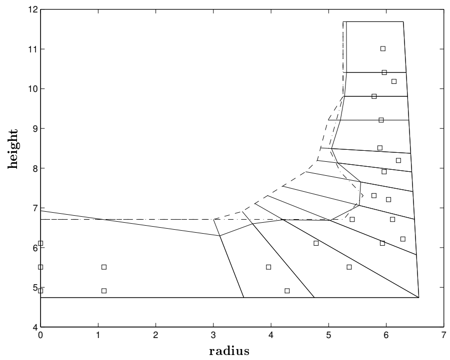

$\alpha = 1225$

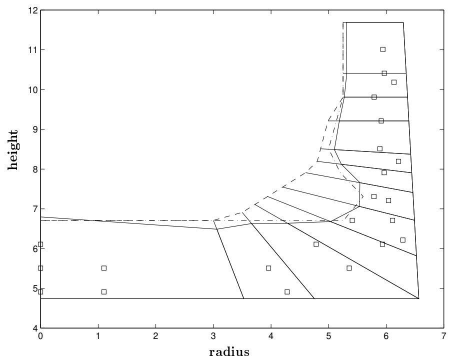

$\alpha = 3025$

Fig. 4. Solutions with simulated data and different regularization parameters, 10% noise

If this replacement is just $\omega \cdot I$, we obtain the (nonlinear damped) *Landweber method*

$$x_{n+1}^\delta = x_n^\delta - \omega F'(x_n^\delta)^*(F(x_n^\delta) - y^\delta), \tag{36}$$

if this replacement is defined via (linear) Tikhonov regularization, we obtain the *Levenberg–Marquardt method*

$$x_{n+1}^\delta = x_n^\delta - [F'(x_n^\delta)^* F'(x_n^\delta) + \alpha_n I]^{-1} F'(x_n^\delta)^*(F(x_n^\delta) - y^\delta); \tag{37}$$

a variant of this method which has slightly better stability properties for ill–posed problems is the *iteratively regularized Gauß–Newton method (IRGN)*

$$\begin{aligned} x_{n+1}^\delta = x_n^\delta - {} & [F'(x_n^\delta)^* F'(x_n^\delta) + \alpha_n I]^{-1} \\ & [F'(x_n^\delta)^*(F(x_n^\delta) - y^\delta) + \alpha_n(x_n^\delta - \zeta)] \end{aligned} \tag{38}$$

with an appropriately chosen a–priori guess ζ.

In [33], a Quasi-Newton method was used for solving the inverse problem numerically. A crucial point there (as often with iterative methods involving F') was the efficient computation of the derivative, which was done using an adjoint problem; see [33] for details and numerical results.

Crucial questions for iterative methods are the choice of the stopping index $n = n(\delta, y^\delta)$ and convergence rates. These have been studied e.g. in [2], [39], [38], [7], [6], [47], [48], [58], [65], [60], [41]. Multilevel iterative methods habe been considered in [64], [66], [32]. In [32], a general approach for analyzing convergence of iterative methods for solving nonlinear ill–posed problems has been developed (see also [31]); this approach is based on invariance principles as they had been used for well–posed problems in [19]. This approach also allows to prove convergence rates under logarithmic source conditions of the type

$$x^\dagger - x_0 = f_p(F'(x^\dagger)^* F'(x^\dagger))w \tag{39}$$

instead of (32) (with x^* replaced by the initial iterate x_0) with

$$f_p(\lambda) = (1 - \ln\lambda)^{-p}, 0 < \lambda \leq 1. \tag{40}$$

Such conditions turn out to be appropriate for severely ill–posed problems for which the forward operator is exponentially smoothing like inverse scattering (see [43], [44]). The resulting convergence rate is logarithmic; e.g.,

$$\|x_{n_*}^\delta - x^\dagger\| = O((-\ln\delta)^{-p}) \tag{41}$$

holds under conditions (39), (40) (and some technical conditions, see [43], [32]) for Landweber iteration and IRGN, if the stopping index n_* is determined via a discrepancy principle

$$\|F(x_{n_*}^\delta) - y^\delta\| \leq C\delta < \|F(x_n^\delta) - y^\delta\|, 0 \leq n < n_* \tag{42}$$

with a suitable $C > 2$.

We close by reporting about the application of Landweber iteration to a parameter identification problem arising in modelling the crystallization of polymers; this provides a link to the survey paper [13] in this volume.

A model for one-dimensional crystallization of polymers leads to initial-boundary value problems of the form

$$\frac{\partial T}{\partial t} = D\frac{\partial^2 T}{\partial x^2} + L\frac{\partial \xi}{\partial t} \tag{43}$$

$$\frac{\partial}{\partial t}\left(\frac{1}{\widetilde{G}(T)(1-\xi)}\frac{\partial \xi}{\partial t}\right) = \frac{\partial}{\partial x}\left(\frac{\widetilde{G}(T)}{1-\xi}\frac{\partial \xi}{\partial x}\right) + 2\frac{\partial}{\partial t}(\widetilde{N}(T)) \tag{44}$$

with initial conditions

$$T(x,0) = T^0(x) \tag{45}$$

$$\xi(x,0) = 0 \tag{46}$$

$$\frac{\partial \xi}{\partial t}(x,0) = 0 \tag{47}$$

and boundary conditions

$$\frac{\partial T}{\partial n}(x,t) = \alpha(T(x,t) - T^1(x,t)) \text{ for } x \in \partial\Omega \tag{48}$$

$$\frac{\partial \xi}{\partial t}(x,t) + \widetilde{G}(T)\frac{\partial \xi}{\partial n}(x,t) = 0 \text{ for } x \in \partial\Omega, \tag{49}$$

where T^1 in (48) represents an exterior temperature in the cooling process at the boundary (see[11]).

In these equations, T denotes the temperature, ξ the degree of crystallinity. The parameters arising in the heat transfer problem, i.e., the diffusion coefficient D, the latent heat L and the heat transition coefficient α, can be determined experimentally. The function $\widetilde{N}$ represents an equivalent nucleation rate per unit of length and $\widetilde{G}$ the radial growth rate of a nucleus. Note that $\widetilde{G}$ and $\widetilde{N}$ depend on temperature rather strongly and cannot (at least not simultaneously) be measured as functions of temperature. Some materials admit experimental determination of the growth rate (cf.[62]), in these cases the identification of $\widetilde{N}$ for known $\widetilde{G}$ is of special interest.

The measurable quantities in usual experiments are the temperature T on the boundary of the crystallization domain Ω (or at least on a part of the boundary $\Gamma \subset \partial\Omega$) as well as the degree of crystallinity $\xi(x,t_*)$ at the end of the process. The temperature at the end of the experiment is not measurable, because the structure is frozen in by a final quench below the melting point.

Via various transformations (see [11]), (44) - (49) can be rewritten as

$$\begin{aligned} u_t &= Du_{xx} + Le^{-v}v_t \\ v_t &= a(u)w \\ w_t &= (a(u)v_x)_x + b(u)_t \end{aligned} \tag{50}$$

$$
\begin{aligned}
&u|_{t=0} = u^0\\
&v|_{t=0} = 0\\
&w|_{t=0} = 0
\end{aligned}
\tag{51}
$$

$$
\begin{aligned}
&u_x(0,t) = -\alpha(u(0,t) - u^1(0,t))\\
&w(0,t) - v_x(0,t) = 0
\end{aligned}
\tag{52}
$$

$$
\begin{aligned}
&u_x(1,t) = 0\\
&v_x(1,t) = 0.
\end{aligned}
\tag{53}
$$

The quantities $a(u)$ and $b(u)$ in (50) are the equivalents to $\widetilde{G}(u)$ and $\widetilde{N}(u)$, transformed to the new reference variable u. The function u is a scaled temperature, i.e., $u = 1$ is above the equilibrium melting point and $u = 0$ below the glass transition temperature, hence the temperature range of interest $[u_1, u_2]$ is a subset of $[0, 1]$. In practice, the temperature at the beginning of the experiment is always above the melting point, i.e., u_2 may be chosen as the melting point. The fact that no nucleation occurs above this temperature implies that $b(u) = 0$ for $u \geq u_2$, so one can assume that $b \in H^1([u_1, u_2])$ and $b(u_2) = 0$.

In [11], it is assumed that the temperature data are given at the point $x = 0$ by $u(0,t) = u_B(t)$ in the time interval $I = (0, t_*)$. From the available observation of ξ at $t = t_*$, one can compute the value v_* for $v|_{t=t_*}$, which can therefore be assumed to be given.

Identification of the nucleation rate $\widetilde{N} = \widetilde{N}(T)$ in (43) - (49) is equivalent to identifying $b = b(u)$ in (50) - (53). Thus, this identification problem can formally be written as the nonlinear operator equation

$$F(b) = (u_B^\delta, v_*^\delta), \tag{54}$$

where u_B^δ and v_*^δ denote noisy measurements of u_B and v_* with noise level δ. The operator F, the *parameter-to-output-map*, maps an admissible value of the parameter b to the values u_B and v_* obtained from solving (50) - (53) with this parameter.

Equation (54) has the abstract from (30). In [11], Landweber iteration (36) is applied to this inverse problem leading to an iteration

$$b^{k+1} = b^k - \omega F'(b^k)^*(F(b^k) - (u_B^\delta, v_*^\delta)). \tag{55}$$

In [11], it is shown how $F'(b^k)^*$ can be computed efficiently by solving a system of linear partial differential equations. For results of Landweber iteration (with the stopping index determined by a discrepancy principle (42)), we refer to [11]. We just quote one Figure, which shows the residual and the error $\|b^k - b^{\text{true}}\|$ versus the iteration number for simulated data with 2 % noise:

The error in Figure 5 shows the same behaviour as predicted by the theory (cf. Figure 3), the stopping index determined by the discrepancy principle is remarkably close to the minimal error; if one iterates beyond this stopping index, the error increases quickly, which is a behaviour one should always keep in mind when solving inverse problems iteratively.

In [10], the iteratively regularized Gauß-Newton method (38) has been applied to the same inverse problem.

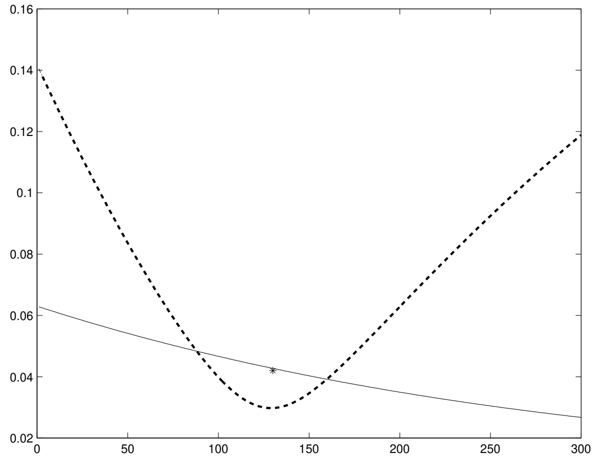

Fig. 5. Residual (solid) and error (dashed) vs. iteration number. The stopping index is marked by $*$.

References

1. G. Backus and F. Gilbert, Numerical applications of a formalism for geophysical inverse problems, *Geophys. J. R. Astron. Soc.*, **13**(1967) 247-276
2. A.B. Bakushinskii, The problem of the convergence of the iteratively regularized Gauß-Newton method, *Comput. Maths. Math. Phys.*, **32**(1992) 1353–1359
3. H. Banks and K. Kunisch, Parameter Estimation Techniques for Distributed Systems, Birkhäuser, Boston, 1989
4. J. Beck, B. Blackwell, C.S. Clair, Inverse Heat Conduction: Ill–Posed Problems; Wiley, New York 1985
5. M. Bertero, P. Boccacci, Introduction to Inverse Problems in Imaging; Inst. of Physics Publ., Bristol 1998
6. B. Blaschke, A. Neubauer, and O. Scherzer, On convergence rates for the iteratively regularized Gauss-Newton method, *IMA J. Numer. Anal.*, **17**(1997) 421–436
7. A. Binder, M. Hanke, and O. Scherzer, On the Landweber iteration for nonlinear ill-posed problems, *J. Inverse Ill-Posed Probl.*, **4**(1996) 381–389
8. A. Binder, H. W. Engl, C. W. Groetsch, A. Neubauer and O. Scherzer, Weakly closed nonlinear operators and parameter identification in parabolic equations by Tikhonov regularization, *Appl. Anal.*, **55**(1994) 215–234
9. H. Brakhage, On ill-posed problems and the method of conjugate gradients, in [24], 165–175
10. M. Burger, Iterative regularization of a parameter identification problem occurring in polymer crystallization, submitted
11. M. Burger, V. Capasso, H.W. Engl, Inverse problems related to crystallization of polymers, *Inverse Problems*, **15** (1999) 155-173

12. M. Burger, H.W. Engl, Training neural networks with noisy data as an ill–posed problem, to appear in *Advances in Comp. Mathematics*
13. V. Capasso, A case study: Mathematics of the polymer crystallization, this volume
14. G. Chavent, K. Kunisch, On weakly nonlinear inverse problems, *SIAM J. Appl. Math.*, **56**(1996) 542–572
15. D. Colton, R. Ewing, and W. Rundell, Inverse Problems in Partial Differential Equations, SIAM, Philadelphia, 1990
16. D. Colton and R. Kress, Inverse Acoustic and Electromagnetic Scattering Theory, Springer, Berlin, 1992
17. D. Colton, A. Kirsch, A simple method for solving inverse scattering problems in the resonance region, *Inverse Problems*, **12**(1996) 383–393.
18. D. Colton, M. Piana, R. Potthast, A simple method using Morozov's discrepancy principle for solving inverse scattering problems, *Inverse Problems*, **13**(1997) 1477-1493
19. P. Deuflhard and G. Heindl, Affine invariant convergence theorems for Newton's method and extensions to related methods, *SIAM J. Numer. Anal.*, **16**(1979) 1–10
20. H. Druckenthaner, H. Zeisel, A. Schiefermüller, G. Kolb, A. Ferstl, H. Engl, A. Schatz, Online simulation of the blast furnace, *Advanced Steel*, (1997-98) 58-61
21. H.W. Engl, Regularization methods for the stable solution of inverse problems, *Surveys on Mathematics for Industry*, **3**(1993) 71–143
22. H. W. Engl and H. Gfrerer, A posteriori parameter choice for general regularization methods for solving linear ill-posed problems, *Appl. Numer. Math.* **4**(1988) 395–417
23. H. W. Engl and W. Grever, Using the L-curve for determining optimal regularization parameters, *Numer. Math.*, **69**(1994) 25–31
24. H. W. Engl and C. W. Groetsch, Inverse and Ill-Posed Problems, Academic Press, Orlando, 1987
25. H. W. Engl, K. Kunisch and A. Neubauer, Convergence rates for Tikhonov regularization of nonlinear ill-posed problems,*Inverse Problems* **5**(1989) 523–540
26. H.W. Engl, T. Langthaler, Control of the solidification front by secondary cooling in continuous casting of steel, in: H.W. Engl, H. Wacker and W. Zulehner, eds. Case Studies in Industrial Mathematics Teubner, Stuttgart, 1988, 51-77
27. H. W. Engl, A. K. Louis and W. Rundell (eds.), Inverse Problems in Geophysics, SIAM, Philadelphia, 1996
28. H. W. Engl, A. K. Louis and W. Rundell (eds.), Inverse Problems in Medical Imaging and Nondestructive Testing, Springer, Vienna, New York, 1996
29. H. W. Engl and W. Rundell (eds.), Inverse Problems in Diffusion Processes, SIAM, Philadelphia, 1995
30. H.W. Engl, M. Hanke, A. Neubauer, Regularization of Inverse Problems, Kluwer Academic Publishers, Dordrecht, 1996
31. H.W. Engl and O. Scherzer, Convergence rates results for iterative methods for solving nonlinear ill–posed problems, to appear in: D. Colton, H.W. Engl, A.K. Louis, J. McLaughlin, W.F. Rundell (eds.), Solution Methods for Inverse Problems, Springer, Vienna/New York, 2000
32. P. Deuflhard, H.W. Engl, and O. Scherzer, A convergence analysis of iterative methods for the solution of nonlinear ill–posed problems under affinely invariant conditions, *Inverse Probl.*, **14**(1998) 1081–1106
33. W. Grever, A. Binder, H.W. Engl, K. Mörwald, Optimal cooling strategies in continuous casting of steel with variable casting speed, *Inverse Problems in Engineering*, **2** (1996) 289-300
34. W. Grever A nonlinear parabolic initial boundary value problem modelling the continuous casting of steel with variable casting speed, *ZAMM*, **78** (1998) 109-119

35. C. W. Groetsch, Inverse Problems in the Mathematical Sciences, Vieweg, Braunschweig, 1993
36. C. W. Groetsch, Generalized Inverses of Linear Operators: Representation and Approximation, Dekker, New York, 1977
37. M. Hanke, Conjugate Gradient Type Methods for Ill-Posed Problems, Longman Scientific & Technical, Harlow, Essex, 1995
38. M. Hanke, A regularizing Levenberg-Marquardt scheme, with applications to inverse groundwater filtration problems. *Inverse Probl.*, **13**(1997) 79–95
39. M. Hanke, A. Neubauer, and O. Scherzer. A convergence analysis of Landweber iteration for nonlinear ill-posed problems, *Numer. Math.*, **72**(1995) 21–37
40. P. C. Hansen and D. P. O'Leary, The use of the L-curve in the regularization of discrete ill-posed problems, *SIAM J. Sci. Comput.*, **14** (1993) 1487–1503
41. F. Hettlich and W. Rundell, The determination of a discontinuity in a conductivity from a single boundary measurement, *Inverse Probl.*, **14**(1998) 67–82
42. B. Hofmann, Mathematik inverser Probleme, Teubner, Stuttgart 1999
43. T. Hohage, Logarithmic convergence rates of the iteratively regularized Gauß–Newton method for an inverse potential and an inverse scattering problem, *Inverse Problems*, **13**(1997) 1279-1299
44. T. Hohage, Convergence rates of a regularized Newton method in sound–hard inverse scattering, *SIAM J. Numer. Anal.*, **36**(1998) 125–142
45. D. Isaacson and J.C. Newell, Electrical Impedance Tomography, *SIAM Review*, **41**(1999) 85–101
46. V. Isakov, Inverse Problems in Partial Differential Equations, Springer, Berlin, New York, 1998
47. B. Kaltenbacher, Some Newton-type methods for the regularization of nonlinear ill-posed problems, *Inverse Probl.*, **13**(1997) 729–753
48. B. Kaltenbacher, A posteriori parameter choice strategies for some Newton type methods for the regularization of nonlinear ill–posed problems, *Numer. Math.*, **79**(1998) 501–528
49. A. Kirsch, An Introduction to the Mathematical Theory of Inverse Problems, Springer, New York 1996
50. A. Kirsch, B. Schomburg and G. Berendt, The Backus-Gilbert method, *Inverse Problems*, **4**(1988) 771–783
51. G. Landl, T. Langthaler, H. W. Engl and H. F. Kauffmann, Distribution of event times in time-resolved fluorescence: the exponential series approach – algorithm, regularization, analysis, *J. Comput. Phys.*, **95**(1991) 1–28
52. A. Leonov and A. Yagola, Special regularizing methods for ill–posed problems with sourcewise represented solutions, *Inverse Problems*, **14**(1998) 1539–1550
53. A. K. Louis, Inverse und schlecht gestellte Probleme, Teubner, Stuttgart, 1989
54. A. K. Louis, Convergence of the conjugate gradient method for compact operators, in [24], 177–183
55. A. K. Louis and P. Maass, A mollifier method for linear operator equations of the first kind, *Inverse Problems*, **6**(1990) 427–440
56. M. Z. Nashed, Generalized Inverses and Applications, Academic Press, New York, 1976
57. F. Natterer, The Mathematics of Computerized Tomography, Teubner, Stuttgart, 1986
58. A. Neubauer and O. Scherzer, A convergence rate result for a steepest descent method and a minimal error method for the solution of nonlinear ill-posed problems, *Z. Anal. Anwend.*, **14**(1995) 369–377

59. E. Radmoser, R. Wincor, Determining the inner contour of a furnace from temperature measurements, Industrial Mathematics Institute, Johannes Kepler Universität Linz, *Technical Report* **12** (1998)
60. R. Ramlau, A modified Landweber-method for inverse problems *Num. Funct. Anal. Opt.*, **20**(1999) 79–98
61. A. Ramm, Scattering by Obstacles, Reidel, Dordrecht, 1986
62. E.Ratajski, H.Janeschitz-Kriegl, How to determine high growth speeds in polymer crystallization, *Colloid Polym. Sci.*, **274** (1996) 938-951
63. T. Raus, Residue principle for ill-posed problems, *Acta et Comment. Univers. Tartuensis*, **672**(1984) 16-26
64. A. Rieder, A wavelet multilevel method for ill-posed problems stabilized by Tikhonov regularization, *Numer. Math.*, **75**(1997) 501–522
65. O. Scherzer, A convergence analysis of a method of steepest descent and a two-step algorithm for nonlinear ill-posed problems, *Numer. Funct. Anal. Optimization*, **17**(1996) 197–214
66. O. Scherzer, An iterative multi level algorithm for solving nonlinear ill–posed problems, *Numer. Math.*, **80**(1998) 579–600
67. E. Schock, Approximate solution of ill-posed equations: arbitrarily slow convergence vs. superconvergence, in: G. Hämmerlin and K. H. Hoffmann, eds., Constructive Methods for the Practical Treatment of Integral Equations, Birkhäuser, Basel, 1985, 234–243
68. T. I. Seidman and C. R. Vogel, Well-posedness and convergence of some regularization methods for nonlinear ill-posed problems, *Inverse Problems*, **5**(1989) 227–238
69. M. Tanaka, T. Matsumoto, S. Oida, Identification of unknown boundary shape of rotationally symmetric body in steady heat conduction via BEM and filter theories, in: M. Tanaka and G.S. Dulikravich eds., Inverse Problems in Engineering Mechanics, Elsevier Science B.V., Tokyo, 1998, 121-130
70. C. R. Vogel, Non-convergence of the L-curve regularization parameter selection method,*Inverse Problems*, **12**(1996) 535–547
71. G. Wahba, Spline Models for Observational Data, SIAM, Philadelphia, 1990

Acknowledgement: Partially supported by the Austrian Science Foundation FWF, projects F 1308 and P13478-INF.